From frustrated insulators to correlated anisotropic metals: charge-ordering and quantum criticality in coupled chain systems

2008 J. Phys.: Condens. Matter 20 235213

(http://iopscience.iop.org/0953-8984/20/23/235213)

J. Phys.: Condens. Matter **20** (2008) 235213 (11pp) doi:10.1088/0953-8984/20/23/235213

From frustrated insulators to correlated anisotropic metals: charge-ordering and quantum criticality in coupled chain systems

Siddhartha Lal[1,3] **and Mukul S Laad**[2]

[1] The Abdus Salam ICTP, Strada Costiera 11, Trieste 34014, Italy
[2] Max-Planck-Institut für Physik Komplexer Systeme, 01187 Dresden, Germany

E-mail: slal@ictp.it and mukul@mpipks-dresden.mpg.de

Received 9 October 2007, in final form 1 March 2008
Published 6 May 2008
Online at stacks.iop.org/JPhysCM/20/235213

Abstract
By following the ideas of Emery and Noguera, a recent study revealed the dynamics of the charge sector of a one-dimensional quarter-filled electronic system with extended Hubbard interactions to be that of an effective pseudospin transverse-field Ising model (TFIM) in the strong-coupling limit. With the twin motivations of studying the co-existing charge and spin order found in strongly correlated chain systems and the effects of interchain couplings, we investigate the phase diagram of coupled effective (TFIM) systems. A bosonization and renormalization group (RG) analysis for a two-leg TFIM ladder yields a rich phase diagram showing Wigner/Peierls charge order and Néel/dimer spin order. In a broad parameter regime, the orbital antiferromagnetic phase is found to be stable. An intermediate gapless phase of finite width is found to lie in between two charge-ordered gapped phases. Kosterlitz–Thouless transitions are found to lead from the gapless phase to either of the charge-ordered phases. A detailed analysis is also carried out for the dimensional crossover physics when many such pseudospin systems are coupled to one another. Importantly, the analysis reveals the key role of critical quantum fluctuations in driving the strong dispersion in the transverse directions, as well as a $T = 0$ deconfinement transition. Our work is potentially relevant for a unified description of a class of strongly correlated, quarter-filled chain and ladder systems.

1. Introduction

Strongly correlated ladder systems are fascinating candidates for studying the interplay of spin and charge ordering, and their combined influence on the emergence of novel ground states [1]. Several recent studies provide experimental realizations of such systems, exhibiting diverse phenomena like charge order (CO), antiferromagnetism (AF) and unconventional superconductivity (uSC) as functions of suitable control parameters [2, 3]. The existence of several non-perturbative theoretical techniques in one dimension has also resulted in the study of the emergence of exotic phases from instabilities of the high-T Luttinger liquid [4]. Given that these systems are Mott insulators, longer-range Coulomb interactions are relevant in understanding CO/AF/uSC phases. Despite some recent work [5], a detailed understanding of the effects of longer-range interactions in quasi-one-dimensional (1D) systems is a largely unexplored problem. Further, attention has mostly focused on studies of models at 1/2-filling [4].

Here, we study an effective pseudospin model describing charge degrees of freedom of a 1D 1/4-filled electronic system. Such an effective model can be derived from an extended Hubbard model (i.e. with longer-range interactions) in a number of physically relevant cases. For example, it is reasonably well established that the structure of the material $Na_2V_2O_5$ is essentially that of a system of weakly coupled quarter-filled two-leg ladders [6–8]. While the spin sector is effectively quasi-1D with each ladder corresponding to a spin chain, the charge sector is well described by a 1D system of

[3] Present address: Department of Physics, University of Illinois at Urbana-Champaign, IL 61801, USA.

Ising pseudospins in a transverse field. The pseudospin degrees of freedom correspond to the position of a localized electron on a given rung of the two-leg ladder.

Another relevant example is the $Sr_{14}Cu_{24}O_{41}$ system, a ladder based material well described by a Hubbard-type fermionic model. Hitherto described by a Hubbard (or extended Hubbard) model at half-filling, recent experimental work by Abbamonte *et al* [9][4] strongly suggests a very new scenario. Since pure $Sr_{14}Cu_{24}O_{41}$ is a Mott insulator with short-ranged antiferromagnetic correlations and a spin gap, nearest neighbour (nn) Coulomb interactions are in fact a necessary ingredient of a minimal model. Additionally, electronic charge–density-wave (e-CDW) order is inferred for zero doping, providing additional evidence for inclusion of nn Coulomb interactions into a minimum effective model for these ladder systems. The e-CDW appears not to be driven by electron–phonon coupling, as shown by the absence of a detectable lattice distortion tied to the e-CDW. The relevance of inter-ladder coupling is also clearly revealed by this study.

Similar arguments hold for the quasi-1D charge transfer organics, which show e-CDW order in the Mott insulating phases in the generalized $T-P$ phase diagram (substitution of different anions in the TMTSF-salts corresponds to varying chemical pressure) [10]. In studying a 1D 1/4-filled fermionic model with extended interactions, it has been suggested [11, 12] that the same Ising pseudospin Hamiltonian may be a relevant starting point for the study of charge-order in organics; we will discuss this in some detail at the start of the following section. Clearly, a half-filled Hubbard (or extended Hubbard) model is inadequate when one seeks to understand Mott insulators with e-CDW (along with AF/dimerized) ground states. A quarter-filled, extended Hubbard model turns out to be a minimal model capable of describing such ground states [13, 14].

While the weak coupling limit of the underlying extended Hubbard model has been recently studied [15, 16], we note that the real systems under consideration are generically in the strong coupling regime of the model [6–8]. To the best of our knowledge, this regime has not been studied in sufficient detail. Another interest is to investigate the conditions under which short-coherence length superconductivity can arise by hole-doping a charge- and antiferromagnetically ordered Mott insulator. Again, this issue has been studied in sufficient detail only in the weak coupling limit [17]. Motivated by the above discussion, we have recently studied a problem of coupled electronic chains [12], where each chain is described by an extended Hubbard model with a hopping term (of strength, t) and nearest-(V_1) and next-nearest neighbour (nnn) (V_2) Coulomb interactions in addition to the local Hubbard (U) interaction [12]. Further, we studied the strong coupling regime, where $U \gg V_1, V_2 \gg t$. In this regime, we derived an effective transverse-field Ising model (TFIM) in terms of pseudospins describing the charge degrees of freedom for a single chain [12]. In this work, our primary aim will be to study the effects of interchain couplings in this system of chains. As noted earlier, it has also been shown in [7] that a quarter-filled two-leg ladder, in which the on-site Coulomb repulsion is the largest coupling, can be mapped onto the same effective TFIM Hamiltonian. Our results will, therefore, also be relevant to an understanding of such ladder systems.

We begin in section 2 by briefly reviewing for the sake of completeness, the derivation of the effective TFIM Hamiltonian for the charge sector of a system of 1/4-filled electronic chains with strong extended Hubbard interactions and very weak nearest neighbour hopping. In this way, we verify explicitly the heuristic ideas of Emery and Noguera [11]. We then proceed with the effective pseudospin TFIM model for the charge degrees of freedom for a single chain [12] and couple neighbouring chains to describe the physical situations detailed above. In this way, a system of two effective pseudospin models coupled to one another is first analysed in section 2 using abelian bosonization and perturbative renormalization group methods, to obtain a rich phase diagram showing different types of CO phases. At the same time, there remains open the intriguing possibility that some of these gapped phases may themselves be separated from one another by non-trivial gapless phases of finite width [18]. We will encounter an example of this phenomenon in section 2.3. The transitions from this gapless critical phase to either of the two charge-ordered phases are found to belong to the Kosterlitz–Thouless universality class. The question that naturally arises is whether such gapless, correlated, anistropic metallic phases survive when many such TFIM systems are coupled to one another so as to undergo a dimensional crossover. To answer this question reliably, we treat the inter-TFIM couplings at the level of the random phase approximation (RPA) [4, 19, 20] in section 3. The finite T neighbourhood of the quantum critical point (QCP) is studied in detail. Interestingly, the inter-TFIM hopping coupling is seen to drive the system away from a gapped phase at $T = 0$ to a gapless one at the QCP: critical quantum fluctuations drive the system through a deconfinement transition together with a dimensional crossover. In section 4, we present a comparison of our findings with some recent numerical works. Finally, we conclude in section 5.

2. Two-leg coupled TFIM ladder model

We begin with the Hamiltonian for a spin chain system

$$H = -\sum_n [t(S_n^x S_{n+1}^x + S_n^y S_{n+1}^y) + V S_n^z S_{n+1}^z + P S_n^z S_{n+2}^z + h S_n^z] \quad (1)$$

where S_n^x, S_n^y and S_n^z are spin-1/2 operators. The couplings $(t, V, P) > 0$ are the nearest neighbour (nn) XY, the nearest neighbour Ising and the next nearest neighbour (nnn) Ising couplings respectively and h is the external magnetic field. For $h = 0$, this Hamiltonian can be derived via a Jordan–Wigner transformation on the charge degrees of freedom of a 1/4-filled extended Hubbard model of electrons on a 1D lattice in the strong-coupling limit: the on-site Hubbard interaction

[4] This paper clearly shows the relevance of inter-ladder coupling for the telephone number compounds. Remarkably, the CO (electronic crystal) is not accompanied by any detectable structural distortion, indicating that electronic correlations, rather than electron–phonon coupling, drive the CO in these systems. This makes it interesting to inquire about the general range of physical manifestations arising in a suitable model as a function of parameters of the model.

$U \rightarrow \infty$, while the nn (V) and nnn (P) density–density interaction couplings and the nn electron hopping (t) are all taken to be finite [12]

$$H = \sum_n \left[-\frac{t}{2}(c_i^\dagger c_{i+1} + \text{h.c.}) + V n_i n_{i+1} + P n_i n_{i+2} \right]. \quad (2)$$

We study the problem in the limit of strong-coupling where $V, P \gg t$ (but where $(V - 2P) \sim 2t$) [12].

Let us begin by studying the case of $t = 0$ [11] (we will be studying equation (1) for the case of $h = 0$ in all that follows). It is easy to see that for the case of $V > 2P$, the ground state of the system is given by a Néel-ordered antiferromagnetic (AF) state with two degenerate ground states given by

$$\begin{aligned} |AFGS1\rangle &= |\cdots + - + - + - + - \cdots\rangle \\ |AFGS2\rangle &= |\cdots - + - + - + - + \cdots\rangle \end{aligned} \quad (3)$$

where we signify $S_n^z = 1/2, -1/2$ by $+$ and $-$ respectively and we have explicitly shown the spin configuration in the site numbers $-3 \leqslant n \leqslant 4$ in the ground states. In the original electronic Hamiltonian equation (2), this AF order corresponds to a Wigner charge-ordering (CO) in the ground state. Similarly, for the case of $V < 2P$, the ground state of the system is given by a dimer-ordered (2, 2) state [11] with four degenerate ground states given by

$$\begin{aligned} |22GS1\rangle &= |\cdots - + + - - + + - \cdots\rangle \\ |22GS2\rangle &= |\cdots - - + + - - + + \cdots\rangle \\ |22GS3\rangle &= |\cdots + - - + + - - + \cdots\rangle \\ |22GS4\rangle &= |\cdots + + - - + + - - \cdots\rangle \end{aligned} \quad (4)$$

where we signify $S_n^z = 1/2, -1/2$ by $+$ and $-$ respectively and we have explicitly shown the spin configuration in the site numbers $-2 \leqslant n \leqslant 5$ in the ground states. In the original electronic Hamiltonian equation (2), this (2, 2) order corresponds to a Peierls CO in the ground state.

The same conclusions for the various ground states of the spin Hamiltonian with $t = 0$ were, in fact, first reached by Emery and Noguera [11]. These authors then reached, through a series of heuristic arguments, the transverse-field Ising model (TFIM) in one dimension as an effective model of the system for the case of small t. In what follows, we provide an explicit derivation of their heuristic conjecture. At the same time, it is important to note that Emery and Noguera [11] were, through a careful numerical investigation, able to substantiate their conjecture. Further, similar methods to those outlined in the remainder of this section have been adopted by the authors of [6, 7] in deriving effective Hamiltonians very similar to the 1D TFIM for related strongly correlated chain and ladder systems. Before proceeding with the derivation, we recount briefly the heuristic arguments of Emery and Noguera [11]. Starting with one of the (2, 2) ground states of the spin Hamiltonian for the case of $t = 0$, Emery and Noguera paired spins into antiparallel pairs and then introduced pseudospins τ such that $\tau^z = 1$ for every $(+, -)$ configuration and $\tau^z = -1$ for every $(-, +)$ configuration. Then, by noting that (a) any one of the four (2, 2) ground states were antiferromagnetically ordered in the τ^z and had a partner obtained by displacement of the state by one bond, and (b) at small and finite t, the XY terms can only flip the τ^z on any bond, they concluded that the Hamiltonian reduced effectively to that of the 1D transverse-field quantum Ising model. As stated above, these heuristic arguments were then verified by the authors by carrying out a careful numerical investigation. As a formal derivation of this conjecture has never been presented, we now fill this lacunae.

Let us now proceed with our derivation. First, we consider the effect of the XY terms in the Hamiltonian (1) on these ground states. Let us start with noting the effect of an XY term on a single nn spin pair on the four degenerate (2, 2) ground states; for purposes of brevity, we will denote the entire $t(S_n^x S_{n+1}^x + Sn^y S_{n+1}^y)$ term simply as $t^{n,n+1}$. Thus,

$$\begin{aligned} t^{0,1}|22GS1\rangle &= t^{0,1}|\cdots + - \cdots\rangle = \frac{t}{2}|\cdots - + \cdots\rangle \\ t^{0,1}|22GS2\rangle &= t^{0,1}|\cdots + + \cdots\rangle = 0 \\ t^{0,1}|22GS3\rangle &= t^{0,1}|\cdots - + \cdots\rangle = \frac{t}{2}|\cdots + - \cdots\rangle \\ t^{0,1}|22GS1\rangle &= t^{0,1}|\cdots - - \cdots\rangle = 0 \\ t^{-1,0}|22GS1\rangle &= t^{-1,0}|\cdots + + \cdots\rangle = 0 \\ t^{-1,0}|22GS2\rangle &= t^{-1,0}|\cdots - + \cdots\rangle = \frac{t}{2}|\cdots + - \cdots\rangle \\ t^{-1,0}|22GS3\rangle &= t^{-1,0}|\cdots - - \cdots\rangle = 0 \\ t^{-1,0}|22GS4\rangle &= t^{-1,0}|\cdots + - \cdots\rangle = \frac{t}{2}|\cdots - + \cdots\rangle. \end{aligned} \quad (5)$$

In a similar manner, we study the action of the operator $t^{n,n+1}$ on the two degenerate ground states of the AF ordered configuration as

$$\begin{aligned} t^{0,1}|AFGS1\rangle &= t^{0,1}|\cdots + - \cdots\rangle = \frac{t}{2}|\cdots - + \cdots\rangle \\ t^{0,1}|AFGS2\rangle &= t^{0,1}|\cdots - + \cdots\rangle = \frac{t}{2}|\cdots + - \cdots\rangle \\ t^{-1,0}|AFGS1\rangle &= t^{-1,0}|\cdots - + \cdots\rangle = \frac{t}{2}|\cdots + - \cdots\rangle \\ t^{-1,0}|AFGS2\rangle &= t^{-1,0}|\cdots + - \cdots\rangle = \frac{t}{2}|\cdots - + \cdots\rangle. \end{aligned} \quad (6)$$

Defining bond-pseudospins $\tau_i^z = (S_i^z - S_{i-1}^z)/2$, $\tau_i^+ = S_i^+ S_{i-1}^-$ and $\tau_i^- = S_i^- S_{i-1}^+$ (which can be rewritten in terms of bond-fermionic operators in the original electronic Hamiltonian equation (2) as $\tau_i^z = (n_i - n_{i-1})/2$, $\tau_i^+ = c_i^\dagger c_{i-1}$ and $\tau_i^- = c_i c_{i-1}^\dagger$ respectively), we can write the four degenerate ground states of the (2, 2) ordered configuration in terms of these bond-pseudospins as

$$\begin{aligned} |22GS1\rangle &= |\cdots 0 - 0 + 0 \cdots\rangle \\ |22GS2\rangle &= |\cdots + 0 - 0 + \cdots\rangle \\ |22GS3\rangle &= |\cdots 0 + 0 - 0 \cdots\rangle \\ |22GS4\rangle &= |\cdots - 0 + 0 - \cdots\rangle, \end{aligned} \quad (7)$$

where we have denoted $\tau_n^z = 1/2$ as $+$ and $\tau_n^z = -1/2$ as $-$ and have explicitly shown the pseudospin configurations on

the bond numbers $0 \leqslant n \leqslant 4$. We can clearly see from equation (7) that these four ground states break up into two pairs of doubly degenerate (AF) orderings of the pseudospins defined on the odd bonds ($|22GS1\rangle$ and $|22GS3\rangle$) and on the even bonds ($|22GS2\rangle$ and $|22GS4\rangle$) respectively. It is also simple to see from equation (5) that the action of the operator $t^{n-1,n}$ (for the nearest neighbour pair of sites given by $(n-1,n)$) on these four ground states is to flip a pseudospin defined on the bond n (lying in between the pair of sites $(n-1,n)$) or to have no effect at all.

We can now similarly see that the two degenerate ground states of the AF ordered configuration can be written in terms of the bond-pseudospins defined above as

$$\begin{aligned} |AFGS1\rangle &= |\cdots + - + - + \cdots\rangle \\ |AFGS2\rangle &= |\cdots - + - + - \cdots\rangle \end{aligned} \tag{8}$$

where we have explicitly shown the pseudospin configurations on the bond numbers $0 \leqslant n \leqslant 4$. From equation (8), we see that the two degenerate ground states have antiferromagnetic ordering of pseudospins on nn bonds; this can equally well be understood in terms of the ferromagnetic ordering of pseudospins on the odd bonds and on the even bonds separately. Further, from equation (6), we can see that the action of the operator $t^{n-1,n}$ (for the nearest neighbour pair of sites given by $(n-1,n)$) on these two ground states is again to flip a pseudospin defined on the odd (even) bond n (lying in between the pair of sites $(n-1,n)$) against a background of ferromagnetically ordered configurations of pseudospins defined on the odd (even) bonds.

Thus, we can model these pseudospin-ordered ground states (7), (8) as well as all possible pseudospin-flip excitations above them (as given by action of operators of the type $t^{n-1,n}$ (5), (6)) with the effective Hamiltonian [12]

$$\begin{aligned} H =& -\sum_{n\in\text{odd}} [2t\tau_n^x + (V-2P)\tau_n^z\tau_{n+2}^z] \\ & - \sum_{n\in\text{even}} [2t\tau_n^x + (V-2P)\tau_n^z\tau_{n+2}^z] \\ =& \sum_n [2t\tau_n^x + (V-2P)\tau_n^z\tau_{n+2}^z]\,, \end{aligned} \tag{9}$$

where n is the bond index.

This is just the Ising model in a transverse field, which is exactly solvable [21, 22] and has been studied extensively in one dimension [1, 23]. If $(V-2P) > 0$, the ground state is ferromagnetically ordered in τ^z, i.e. it corresponds to a Wigner CDW. For $(V-2P) < 0$, the Peierls dimer order results in the ground state. At $(V-2P) < 2t$, the quantum disordered phase has short-ranged pseudospin correlations, and is a charge 'valence-bond' liquid. The quantum critical point at $(V-2P) = 2t$ separating these phases is a deconfined phase with gapless pseudospin (τ) excitations, and power-law fall-off in the pseudospin–pseudospin correlation functions. Correspondingly, the density–density correlation function has a power-law singular behaviour at low energy, with an exponent $\alpha = 1/4$ characteristic of the 2D Ising model at criticality. The gap in the pseudospin spectrum on either side of the critical point is given by $\Delta_\tau = 2|V-2P-2t|$. Further, the quantum critical behaviour extends to temperatures as high as $T \sim \Delta_\tau/2$ [24] and undergoes finite-temperature crossovers to the two gapped phases at $T \sim |\Delta_\tau|$. The dynamics of the spin sector of a 1/4-filled electronic system in the limit of strong correlations was also studied in [12]; we restrict ourselves to a few brief remarks on the spin sector in this work and direct the reader to [12] for more details. Henceforth, we will focus primarily on the effects of interchain couplings on the charge sector of such chain systems.

2.1. Bosonization and RG analysis

Thus, we now proceed with the effective pseudospin Hamiltonian for the charge sector

$$H^{\text{chain}} = -\sum_j [2t\ \tau_j^x + (V-2P)\ \tau_j^z\tau_{j+1}^z] \tag{10}$$

where the Ising pseudospin coupling $V-2P$ has been replaced by V for convenience in all that follows. Note that since the effective Hamiltonian (9) involves couplings between only the nearest neighbours in either the odd or even sublattices respectively, the site index j in equation (10) is taken as belonging to a particular sublattice and the sum over the two sublattices is then taken separately. While selecting the relevant interchain couplings to consider, it is natural to return to the original electronic problem. Keeping in mind the fact that the single-particle interchain electron transfer process is renormalization group (RG) irrelevant for sufficiently large and extended electronic interactions [4], we note that two-particle interchain density–density couplings as well as electron transfer processes can still be very important. Therefore, by first rotating the pseudospin axis $\tau^x \rightarrow \tau^z$, $\tau^z \rightarrow -\tau^x$, we introduce a bond-fermion repulsion $U_\perp \sum_{i,a,b\neq a}(n_{i,a} - n_{i+1,a})(n_{i,b} - n_{i+1,b})$ as well as a bond-fermion transfer term $t_\perp \sum_{i,a,b\neq a}(c^\dagger_{i,a,\uparrow}c_{i+1,a,\uparrow}c^\dagger_{i,b,\downarrow}c_{i+1,b,\downarrow} +$ h.c.) between two such chain systems described by the indices (a,b). Further, from the explicit construction of these terms, it is also clear that they connect both the nearest neighbour as well as next nearest neighbour sites connecting the two neighbouring chains in the original electronic problem. Recalling the relations between the pseudospins and the bond-fermions in the original electronic model given earlier below equation (6), we can write the effective Hamiltonian for the charge sector of the coupled system in terms of a pseudospin ladder model

$$\begin{aligned} H =& -\sum_{j,a} [2t\ \tau_{j,a}^z + V\ \tau_{j,a}^x\tau_{j+1,a}^x] \\ & - \sum_{j,a,b\neq a} [U_\perp\tau_{j,a}^z\tau_{j,b}^z + t_\perp\ (\tau_{j,a}^x\tau_{j,b}^x + \tau_{j,a}^y\tau_{j,b}^y)]\,, \end{aligned} \tag{11}$$

where $a, b = 1, 2$ is the chain index. Having explored the strong-coupling limit of $U_\perp \gg V$ in an earlier work [12], we will explore the weak-coupling scenario of $U_\perp \ll V$ below. We note that in the spin sector, coupling between the two systems leads to a $S = 1/2$ Heisenberg ladder-type model, and this has been studied extensively by several authors [4, 18]. Interchain spin coupling turns out to be relevant, opening up a spin gap: in this case two possibilities are known to result. The ground state has either short-ranged antiferromagnetic

correlations (RVB) with no magnetic long-range order (LRO), or it spontaneously breaks translation symmetry, leading to dimerization.

We now return to our analysis of the charge sector. To begin, we introduce fermionic operators $\psi_{j,a}$ on each chain via a Jordan–Wigner transformation of the pseudospins. We will then proceed to bosonize the theory. During this procedure, one has to take care that the spin commutation relations are maintained, i.e. the new fermionic operators have anticommutation relations on each chain but commute between chains. It can indeed be checked that the bosonized expression for the various pseudospin operators satisfy the required spin commutation relations [4, 25]. In terms of these fermions, upon denoting the chains as $a, b = \uparrow, \downarrow$, we find an effective Hamiltonian for the 1D Hubbard model with an equal-spin pairing term and an on-site spin-flip term

$$\begin{aligned} H = &-\frac{\tilde{t}}{2}\sum_{j,a}(\psi^{\dagger}_{j,a}\psi_{j+1,a} + \text{h.c.}) - \frac{t_{\perp}}{2}\sum_{j}(\psi^{\dagger}_{j,a}\psi_{j,b} + \text{h.c.}) \\ &+ \tilde{U}\sum_{j} n_{j,\uparrow}n_{j,\downarrow} + \tilde{V}\sum_{j,a}(\psi^{\dagger}_{j,a}\psi^{\dagger}_{j+1,a} + \text{h.c}) \\ &+ \mu\sum_{j,a} n_{j,a} \end{aligned} \tag{12}$$

where $\tilde{t}$ and $t_{\perp}$ are the in-chain and interchain hopping parameters respectively, $\mu = -2t$ the chemical potential of the effective model (and unrelated to the filling of the underlying electronic model), $\tilde{U} = -U_{\perp}$ the on-site (Hubbard) interaction coupling and $\tilde{V} = V/4$ the pairing strength. Note that while we treat the parameters $\tilde{t}$ and $\tilde{V}$ as independent parameters for the sake of generality, $\tilde{t} = \tilde{V} = V$ in our original model (11). Bosonizing in the usual way (in terms of the usual charge $\rho = \uparrow + \downarrow$ and spin $\sigma = \uparrow - \downarrow$ variables), we obtain the effective low-energy bosonic Hamiltonian

$$\begin{aligned} H = &\frac{1}{2\pi}\int \mathrm{d}x \left[v_{\rho}K_{\rho}(\pi\Pi_{\rho}(x))^2 + \frac{v_{\rho}}{K_{\rho}}(\partial_x\phi_{\rho}(x))^2\right] \\ &+ \frac{1}{2\pi}\int \mathrm{d}x \left[v_{\sigma}K_{\sigma}(\pi\Pi_{\sigma}(x))^2 + \frac{v_{\sigma}}{K_{\sigma}}(\partial_x\phi_{\sigma}(x))^2\right] \\ &+ \frac{U_{\sigma}}{2\pi\alpha}\int \mathrm{d}x\cos(\sqrt{8}\phi_{\sigma}) + \frac{U_{\rho}}{2\pi\alpha}\int \mathrm{d}x\cos(\sqrt{8}\phi_{\rho}) \\ &+ \frac{\tilde{V}}{2\pi\alpha}\int \mathrm{d}x\cos(\sqrt{2}\theta_{\rho})\cos(\sqrt{2}\theta_{\sigma}) \\ &- \frac{\sqrt{2}\mu}{\pi}\int \mathrm{d}x\,\partial_x\phi_{\rho}(x) \\ &+ \frac{t_{\perp}}{\pi\alpha}\int \mathrm{d}x\cos(\sqrt{2}\phi_{\sigma})\cos(\sqrt{2}\theta_{\sigma}) \\ &+ \frac{V_1}{\pi\alpha}\int \mathrm{d}x\cos(\sqrt{8}\theta_{\sigma}) \\ &+ \frac{V_2}{\pi\alpha}\int \mathrm{d}x\cos(\sqrt{2}\phi_{\sigma})\cos(\sqrt{2}\theta_{\rho}) \end{aligned} \tag{13}$$

where $\Pi_{\rho} = \frac{1}{\pi}\partial_x\theta_{\rho}$, $\Pi_{\sigma} = \frac{1}{\pi}\partial_x\theta_{\sigma}$, $v_{\rho}K_{\rho} = v_F = v_{\sigma}K_{\sigma}$, $v_{\rho}/K_{\rho} = v_F(1 + \frac{\tilde{U}}{\pi v_F})$ and $v_{\sigma}/K_{\sigma} = v_F(1 - \frac{\tilde{U}}{\pi v_F})$. Among the various cosine potentials, we have the usual spin-flip backscattering $\cos(\sqrt{8}\phi_{\sigma})$ and Umklapp $\cos(\sqrt{8}\phi_{\rho})$ terms as well as the triplet superconducting $\cos(\sqrt{2}\theta_{\rho})\cos(\sqrt{2}\theta_{\sigma})$ term. The chemical potential term can be absorbed by performing the shift $\phi_{\rho} \to \phi_{\rho} + \frac{\sqrt{2}K_{\rho}\mu}{v_{\rho}}x$. The cosine potentials with couplings V_1 and V_2 are generated under RG by the $t_{\perp}$ and $\tilde{V}$ terms. Using the operator product expansion [4], we find the RG equations for the various couplings to second order as

$$\begin{aligned} \frac{\mathrm{d}U_{\rho}}{\mathrm{d}l} &= \left(2 - 2K_{\rho}\right)U_{\rho} \\ \frac{\mathrm{d}U_{\sigma}}{\mathrm{d}l} &= (2 - 2K_{\sigma})\,U_{\sigma} - \left(\frac{1}{K_{\sigma}} - K_{\sigma}\right)t_{\perp}^2 \\ \frac{\mathrm{d}\tilde{V}}{\mathrm{d}l} &= \left(2 - \frac{1}{2}\left(\frac{1}{K_{\sigma}} + \frac{1}{K_{\rho}}\right)\right)\tilde{V} - K_{\sigma}t_{\perp}V_2 \\ \frac{\mathrm{d}t_{\perp}}{\mathrm{d}l} &= \left(2 - \frac{1}{2}\left(K_{\sigma} + \frac{1}{K_{\sigma}}\right)\right)t_{\perp} - \frac{\tilde{V}V_2}{K_{\rho}} - \left(K_{\sigma}U_{\sigma} + \frac{V_1}{K_{\sigma}}\right)2t_{\perp} \\ \frac{\mathrm{d}V_1}{\mathrm{d}l} &= \left(2 - \frac{2}{K_{\sigma}}\right)V_1 + \left(\frac{1}{K_{\sigma}} - K_{\sigma}\right)t_{\perp}^2 \\ \frac{\mathrm{d}V_2}{\mathrm{d}l} &= \left(2 - \frac{1}{2}\left(K_{\sigma} + \frac{1}{K_{\rho}}\right)\right)V_2 - \frac{t_{\perp}\tilde{V}}{K_{\sigma}}, \end{aligned} \tag{14}$$

where all couplings have been normalized with respect to the quantity $2\pi v_F$, and we have set $2\pi v_F = 1$ for notational simplicity. The RG equations for the two interaction parameters (K_{ρ}, K_{σ}), the two velocities (v_{ρ}, v_{σ}) as well as the parameter $\delta = K_{\rho}\mu/v_{\rho}$ are found to be

$$\begin{aligned} \frac{\mathrm{d}K_{\sigma}}{\mathrm{d}l} &= -K_{\sigma}^2(U_{\sigma}^2 + V_2^2 + t_{\perp}^2) + V_1^2 + t_{\perp}^2 + \tilde{V}^2 \\ \frac{\mathrm{d}K_{\rho}}{\mathrm{d}l} &= -K_{\rho}^2U_{\rho}^2J_0(\delta(l)\alpha) + V_2^2 + \tilde{V}^2 \\ \frac{\mathrm{d}v_{\sigma}}{\mathrm{d}l} &= -v_{\sigma}K_{\sigma}(U_{\sigma}^2 + V_2^2 + t_{\perp}^2) + \frac{v_{\sigma}}{K_{\sigma}}(V_1^2 + t_{\perp}^2 + \tilde{V}^2) \\ \frac{\mathrm{d}v_{\rho}}{\mathrm{d}l} &= -v_{\rho}K_{\rho}U_{\rho}^2J_2(\delta(l)\alpha) + \frac{v_{\rho}}{K_{\rho}}(V_2^2 + \tilde{V}^2) \\ \frac{\mathrm{d}\delta}{\mathrm{d}l} &= \delta(l) - U_{\rho}^2J_1(\delta(l)\alpha)\,, \end{aligned} \tag{15}$$

where $\delta(l) = \delta e^l$, α is a short-distance cut-off like the lattice spacing and $J_0(x)$ and $J_1(x)$ are Bessel functions [4]. The various second-order correction terms arise from $(\partial_x\phi_{\rho/\sigma})^2$ and $(\partial_x\theta_{\rho/\sigma})^2$, which are generated under the RG transformations [4, 26, 27]. As discussed in [27], the competing influences of the various couplings on the renormalizations of the interaction parameters (K_{ρ}, K_{σ}) can cause their values to either grow or decrease. In turn, this affects drastically the scaling dimensions of the various couplings and can lead to the system undergoing a transition from one type of ordered phase (in which a particular coupling grows the fastest to strong-coupling) to another, with the passage being through a gapless (critical) phase. The existence of such a critical (gapless) region in coupling space, lying in between two ordered (massive) phases, is revealed in a subsequent analysis. Further, such a deconfined phase can be thought of as the quasi-1D analogue of that analysed in detail later via an RPA treatment when dealing with many coupled chains.

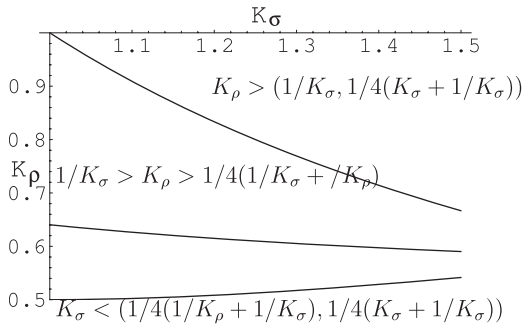

Figure 1. The RG phase diagram in the (K_σ, K_ρ) plane for repulsive interchain interactions ($U_\perp < 0$). The three regions $K_\rho < (1/4\ (1/K_\sigma + 1/K_\rho), 1/4\ (K_\sigma + 1/K_\sigma))$, $1/K_\sigma > K_\rho > 1/4\ (1/K_\sigma + 1/K_\rho)$ and $K_\rho > (1/K_\sigma, 1/4\ (K_\sigma + 1/K_\sigma))$ give the values of (K_σ, K_ρ) for which the couplings U_ρ, $t_\perp$ and $\tilde{V}$ respectively are the fastest to grow under RG.

2.2. Phase diagram for repulsive inter-TFIM coupling

For repulsive interactions ($U_\perp > 0$) between the bond-fermions, the σ sector is massless and K_σ flows under RG to the fixed point value $K_\sigma^* \gtrsim 1$ and $1/2 \leqslant K_\rho \leqslant 1$. At 1/2-filling (for the bond-fermions), the couplings U_ρ, $\tilde{V}$, $t_\perp$, V_1 and V_2 are all relevant while U_σ is irrelevant. The competition to reach strong-coupling first is, however, mainly between U_ρ, $t_\perp$ and $\tilde{V}$. We show below the phase diagram as derived from this analysis.

In the phase diagram in figure 1, the three lines with intercepts at $(K_\sigma = 1, K_\rho = 1)$, $(K_\sigma = 1, K_\rho = 0.64)$ and $(K_\sigma = 1, K_\rho = 1/2)$ are the relations $K_\sigma = 1/K_\rho$, $K_\rho = 1/4(1/K_\sigma + 1/K_\rho)$ and $K_\rho = 1/4(K_\sigma + 1/K_\sigma)$ respectively. In all that follows, we use the notation $a > (b, c)$ to mean that the quantity a is greater than both the quantities b and c. The regions $K_\rho < (1/4(1/K_\sigma + 1/K_\rho), 1/4(K_\sigma + 1/K_\sigma))$, $1/K_\sigma > K_\rho > 1/4(1/K_\sigma + 1/K_\rho)$ and $K_\rho > (1/K_\sigma, 1/4(K_\sigma + 1/K_\sigma))$ signify the values of K_ρ and K_σ for which U_ρ (in-chain Wigner charge-ordered Mott insulator), $t_\perp$ and $\tilde{V}$ (in-chain Peierls charge-ordered Mott insulator of preformed bond-fermion pairs) respectively are the fastest to reach strong-coupling. The RG equations for the coupling U_ρ, the interaction parameter K_ρ and the incommensuration parameter δ are familiar from the literature on commensurate–incommensurate transitions [28]. For temperatures $T \gg K_\rho \mu$, the finite chemical potential (arising from the non-zero transverse-field strength t) is unable to quench the Umklapp scattering processes, allowing for the growth of U_ρ to strong-coupling. For $T \ll K_\rho \mu$, the finite chemical potential cuts-off the RG flow of U_ρ, freezing the Umklapp scattering processes.

For the case of $t_\perp$ being the most relevant coupling, we find our RG equations to be a non-trivial generalization of those derived in [29] for the model of two coupled spinless fermion chains without the intrachain $\tilde{V}$ pairing term. The resulting picture then describes strong interchain two-particle correlations between bond-fermions sharing a rung. Following the analysis outlined in [29, 18], we conclude that this phase is a novel insulating phase characterized by a mass gap and delocalized bond-fermions on rungs, resembling the orbital antiferromagnetic ground state found in the spinless two-chain problem. This matches our finding of an orbital antiferromagnetic ground state in the strongly coupled ladder with dominant antiferromagnetic rung-couplings in an earlier work [12]. Away from 1/2-filling (for the bond-fermions), the competition is mainly between $t_\perp$ and $\tilde{V}$. For $\tilde{V}$ reaching strong-coupling ahead of $t_\perp$, the system is in a channel triplet-spin singlet superconducting phase with mobile intrachain hole pairs; for $t_\perp$ reaching strong-coupling ahead of $\tilde{V}$, we are currently unable to describe in more detail the dominant instability away from the orbital antiferromagnetism-like insulating phase.

2.3. Gapless phase driven by inter-TFIM hopping

Interestingly, while studies of ladder models have shown a plethora of charge and spin-ordered gapped phases [4, 15, 16], there remains the intriguing possibility that some of these gapped phases may themselves be separated from one another by non-trivial gapless phases of finite width [18]. In what follows, we provide an explicit realization of this scenario. The RG equations (14) and (15) reveal the existence of a non-trivial fixed point (FP) for any value of (K_ρ, K_σ) lying in the ranges $1/2 < K_\rho < 1$, $1 < K_\sigma < 2 + \sqrt{3}$ and which is perturbatively accessible from the trivial weak-coupling FP. While the perturbative RG is known to have its limitations in such cases, the finding of a non-trivial FP is nevertheless reliable as long as the values of the various couplings at the FP are small (as indicated above). We note that a similar non-trivial fixed point was found in a study of the anisotropic Heisenberg spin-1/2 chain in a magnetic field [30], where the authors derived a set of RG equations which were very similar to those found in [29]. Here, the non-trivial FP is given by

$$t_\perp^* = \sqrt{ab}, \qquad V_1^* = \frac{K_\sigma^* + 1}{2} t_\perp^{*2}, \qquad U_\sigma^* = \frac{V_1^*}{2K_\sigma^*}$$
$$\tilde{V}^* = \sqrt{aK_\rho^*(cK_\sigma^* - (K_\sigma^* + 1)^2 ab)}, \qquad V_2^* = \sqrt{\frac{b}{a}}\frac{\tilde{V}^*}{K_\sigma^*} \tag{16}$$

where $a = 2 - (K_\sigma^* + 1/K_\rho^*)/2$, $b = 2 - (1/K_\sigma^* + 1/K_\rho^*)/2$ and $c = 2 - (K_\sigma^* + 1/K_\sigma^*)/2$. Further, we can safely make the approximation of the renormalizations of K_ρ and K_σ being small at this non-trivial FP [30]. The system is gapless at this non-trivial FP as well as at points which flow to it. The trivial FP has six unstable directions (U_ρ, $\tilde{V}$, $t_\perp$, V_1, V_2 and δ), one stable direction (U_σ) and two marginal directions (K_ρ and K_σ). The non-trivial FP has five unstable directions, two stable directions and two marginal directions. The presence of the two stable directions at the non-trivial FP indicates the existence of a two-dimensional surface of gapless theories in the five-dimensional $(U_\sigma, \tilde{V}, t_\perp, V_1, V_2)$ coupling space. This gapless phase is the analogue of the 'Floating Phase' found in the phase diagram of the 1D axial nnn Ising model [30]. We present in figure 2 below an RG flow phase diagram which is projected onto the $(V_1, t_\perp)$ plane (a similar RG flow diagram is found for the case of the anisotropic Heisenberg model in a magnetic field h [30] in the (a, h) plane, where a is the anisotropy parameter).

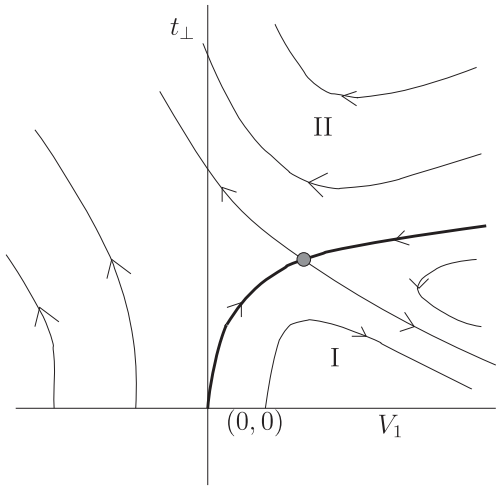

Figure 2. The RG phase diagram in the $(V_1, t_\perp)$ plane. The thick line characterizes the set of points which flow to the intermediate fixed point $(V_1^*, t_\perp^*)$ shown by the filled circle. The thin lines show all RG flows which flow towards strong-coupling in the two phases **I** and **II**, characterized by the relevant couplings $\tilde{V}$ and $t_\perp$ respectively.

The regions **I** and **II** characterize all RG flows which do not flow to the intermediate FP at $(V_1^*, t_\perp^*)$. The transitions from the non-trivial FP towards either of phases **I** and **II** fall under the universality class of the Kosterlitz–Thouless type [30]. In region **I**, V_1 flows to strong-coupling while $t_\perp$ decays; for $1/2 < K_\rho < 1$ and $K_\sigma > 1$, we know from the above discussion that in this region, the coupling $\tilde{V}$ will reach strong-coupling first. In region **II**, both $t_\perp$ and V_1 grow under RG, with the coupling $t_\perp$ being the first to reach strong-coupling. Thus, the RG trajectory leading to the intermediate fixed point represents a gapless phase separating the two gapped, charge-ordered phases **I** and **II** characterized by the relevant couplings $\tilde{V}$ and $t_\perp$ respectively. Nonperturbative insight on such critical phases is also gained in section 4, when we treat the case of many such TFIM systems coupled to one another using the RPA method.

2.4. Phase diagram for attractive inter-TFIM coupling

For attractive interactions ($U_\perp < 0$) between the bond-fermions, we can carry out a similar analysis. In this case, we can see that $K_\rho > 1$ while $K_\sigma < 1$. Then, from the RG equations given above, we can see that the Umklapp couplings U_ρ and V_1 are irrelevant while the couplings $t_\perp$, U_σ, $\tilde{V}$ and V_2 are relevant. The competition to reach strong-coupling first is, however, mainly between U_σ, $t_\perp$ and $\tilde{V}$. We show below the phase diagram at 1/2-filling for the bond-fermions as derived from this analysis.

In the phase diagram in figure 3, the three lines with intercepts at $(K_\rho = 1, K_\sigma = 1)$, $(K_\rho = 1, K_\sigma = 0.64)$ and $(K_\rho = 1, K_\sigma = 1/\sqrt{3})$ are the relations $K_\sigma = 1/K_\rho$, $K_\sigma = 1/4(1/K_\sigma + 1/K_\rho)$ and $K_\sigma = 1/\sqrt{3}$ respectively. The regions $K_\sigma < (1/4(1/K_\sigma + 1/K_\rho), 1/\sqrt{3})$, $1/K_\rho > K_\sigma > 1/\sqrt{3}$ and $K_\sigma > (1/K_\rho, 1/4(1/K_\rho + 1/K_\sigma))$ signify the values of K_ρ and K_σ for which U_σ (rung-dimer insulator with in-chain

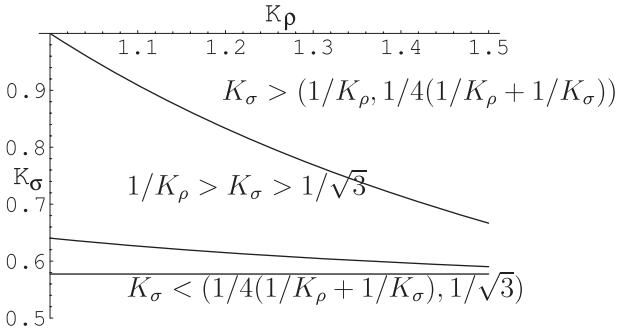

Figure 3. The RG phase diagram in the (K_ρ, K_σ) plane for attractive interchain interactions ($U_\perp > 0$). The three regions $K_\sigma < (1/4(1/K_\sigma + 1/K_\rho), 1/\sqrt{3})$, $1/K_\rho > K_\sigma > 1/\sqrt{3}$ and $K_\sigma > (1/K_\rho, 1/4(1/K_\rho + 1/K_\sigma))$ give the values of (K_σ, K_ρ) for which the couplings U_σ, $t_\perp$ and $\tilde{V}$ respectively are the fastest to grow under RG.

Wigner charge-ordering), $t_\perp$ and $\tilde{V}$ (insulator with in-chain dimers and Peierls charge-ordering) respectively are the fastest to reach strong-coupling. This matches our finding of a ground state with in-chain Wigner charge order and rung-dimers in the strongly coupled ladder with large ferromagnetic rung-couplings in an earlier work [12]. Away from 1/2-filling (for the bond-fermions), depending on which of the three couplings $t_\perp$, $\tilde{V}$ and U_σ is the first to reach strong-coupling, the system exists either as a superconductor with intrachain hole pairs ($\tilde{V}$) or a superconductor with rung-singlet hole pairs (U_σ) or a phase reached by following the dominant instability away from the orbital antiferromagnetism-like insulating phase ($t_\perp$) but which we are currently unable to describe in greater detail.

3. Coupled TFIM systems: quantum criticality, dimensional crossover and deconfinement

Having studied the rich phase diagram of a two-leg coupled TFIM system in the preceding section in considerable detail, we now proceed to investigate the case when many such TFIM systems are coupled to one another. This is done with an effort towards gaining an understanding of how such coupled systems undergo a dimensional crossover from nearly isolated quasi-1D TIFM systems to an anisotropic strongly coupled system in higher dimensions. Dimensional crossover in coupled spin systems has been studied using RG arguments [31, 4] and the RPA for Ising chains [32, 19], Heisenberg chains [20, 33, 4] and ladders in a magnetic field [34] and ladders with frustration [35]. Having used perturbative RG arguments in exploring the phase diagram of the two-leg system earlier, we now employ the RPA method to study the passage to higher dimensionality. This is in keeping with the fact that dimensional crossover is essentially a nonperturbative phenomenon [4]. At the same time, while the mean-field-like approach of RPA is exact only in infinite dimensions (i.e. infinite coordination number), its application to the physics of coupled quasi-1D spin systems for small coordination numbers (i.e. lower dimensions) has met with success [36, 37]. It is also worth noting that while a

naive mean-field treatment of single-particle hopping between fermionic chains is not possible as a single fermion operator has no well-defined classical limit [4], we are able to treat two-particle hopping processes between our underlying chain systems [12] (or, ladder systems [7, 6, 8]) via RPA by working with an effective theory in terms of pseudospins (as evidenced by the inter-chain bond-fermion hopping processes studied earlier for the case of the two-leg ladder). This is justified because the presence of the large on-site Hubbard coupling in our underlying model makes the single-particle hopping irrelevant (in an RG sense) while two-particle processes (including hopping terms) can be crucial in determining the phase diagram [4]. A full treatment including single-particle hopping will require using chain-dynamical mean-field theory (c-DMFT) [38] and will be the focus of a future work. In what follows, we will follow instead the RPA method outlined in [19].

We treat the dynamics of the coupled spin system for the two inter-TFIM couplings, $U_\perp$ and $t_\perp$, in equation (11) given above using the RPA method in turn. Beginning with the coupling $t_\perp$, this method involves computing the dynamical spin susceptibility χ of the coupled system in the disordered phase as

$$\chi(\omega, k, \vec{k}_\perp) = [\chi_{1D}^{-1}(\omega, k) - t_\perp(\vec{k}_\perp)]^{-1} \tag{17}$$

in terms of the frequency ω, the longitudinal and transverse wavevectors k and $\vec{k}_\perp$ respectively. χ_{1D} is the dynamical spin susceptibility of a single TFIM system, to be calculated assuming incipient order along the τ^x direction in pseudospin space

$$\chi_{1D}(\omega, k) = -\mathrm{i}\sum_n \int_0^\infty \mathrm{d}t\, \mathrm{e}^{\mathrm{i}(\omega t - kn)} \langle [\tau^x(t, n), \tau^x(0, 0)] \rangle \tag{18}$$

and the transverse coupling $t_\perp(\vec{k}_\perp) \sim z_\perp t_\perp(\vec{k}_\perp = 0)$, for each TFIM system having a coordination number of $z_\perp$. Then, a divergence in the dynamical pseudospin correlation function $\chi(\omega, k, \vec{k}_\perp)$ signifies an instability towards the formation of an ordered state. However, before setting out with the calculations, it is worth pausing to consider first the likely effects of a transverse coupling like $t_\perp$. As discussed earlier, the phase diagram at $T = 0$ and $t_\perp = 0$ is simple, with an ordered phase for $2t < V$ ($g = (2t - V)/V < 0$), a quantum disordered phase for $2t > V$ ($g > 0$) and a quantum critical point at $2t = V$ ($g = 0$). A finite $t_\perp$ will cause the ordered phase to be extended to finite temperatures (with a critical temperature T_c for the case of $2t = V$), with a first-order phase boundary ending at a new quantum critical point (QCP) $g_c = \Delta_c/V$ at $T = 0$ [19]. As for the simple TFIM [1], there exists a 'quantum critical' region just above the QCP and to the right of the ordered phase, with a crossover to the disordered phase at finite T. This is shown schematically in the T–g phase diagram given below in figure 4. The transition belongs to the 3D Ising universality class while the QCP belongs to the 4D Ising universality class [39].

In the following, we compute, via the RPA method, the quantities g_c at $T = 0$, T_c for the case of $g \equiv \Delta/V = 0$, the shape of the phase boundary near the QCP, the dynamical

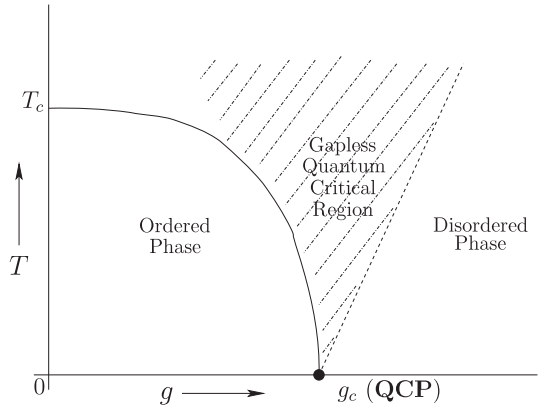

Figure 4. The T–g phase diagram for the case of many TFIM systems coupled by a transverse coupling $t_\perp$ (or $U_\perp$). The $T = 0$ ordered phase of the uncoupled TFIM is now extended, with a phase boundary which has a value T_c for the model at $g = 0$ and a $T = 0$ quantum critical point (QCP) at $g \equiv g_c$. The hashed region immediately to the right of the ordered phase and just above the QCP is the gapless quantum critical region (described in the text). The dashed line represents a finite T crossover from the quantum critical region to a disordered phase.

spin susceptibility $\chi(\omega, k, \vec{k}_\perp)$ at the QCP as well as the dispersion in the transverse directions for small $t_\perp$ and close to the QCP [19]. We focus our attention mainly on, and in the neighbourhood of, the QCP in order to stress the role played by the critical quantum fluctuations in determining the physics of deconfinement and dimensional crossover in our system. In this, we are aided by the integrability and conformal invariance of the TFIM model for $2t = V$, $t_\perp = 0$ [21, 22, 1]; this allows us to exploit the nonperturbative results for a single TFIM system (as long as $\Delta = |2t - V| \ll 1$), while dealing with the physics of the transverse couplings at a mean-field level. At the same time, the spectrum and dispersion deep inside the ordered phase also proves to be fascinating [19]. Specifically, it has been demonstrated that far from the transition line, dispersion in the transverse directions is very weak (i.e. the spectrum is nearly one-dimensional), and a hidden E_8 symmetry of the underlying exactly solvable model [40] gives rise to a spectrum of eight massive particles (three of which should be experimentally observable).

We begin by computing the critical value of the transverse coupling g_c at $T = 0$. For this, we can use the expression for slightly off-critical χ_{1D} for the case when the mass of the single TFIM system is very small ($m = \Delta_c \ll 1$). This, for small ω, is given by

$$\chi_{1D}(\omega, k) \simeq \frac{Z_0 V(\Delta_c/V)^{1/4}}{\omega^2 - (vk)^2 - \Delta_c^2} \tag{19}$$

where the velocity $v = V\alpha$ (where α is the lattice spacing) and $Z_0 = 1.8437$. Then, from the divergence of the susceptibility of the coupled system, $\chi(\omega, k, \vec{k}_\perp)$

$$\chi_{1D}^{-1}(\omega, k) = z_\perp t_\perp(\vec{k}_\perp = 0), \tag{20}$$

we get, for the case of $\omega = 0 = k$,

$$\frac{V}{Z_0} g_c^{7/4} \approx z_\perp t_\perp \tag{21}$$

where we have dropped the argument of $\vec{k}_\perp = 0$ in $t_\perp$ for the sake of convenience. Thus, we get

$$g_c \approx c_1 \left(\frac{z_\perp t_\perp}{V}\right)^{4/7} \tag{22}$$

where the constant $c_1 = Z_0^{4/7} = 1.42$. Precisely the same expression for the mass in the ordered phase and very close to the QCP, $\Delta = g_c V$, is also obtained by carrying out a self-consistent treatment of the effective magnetic field, $h = z_\perp t_\perp \langle \tau^x \rangle$ in the TFIM for a single chain. For this, one uses the slightly off-critical susceptibility for the 1D TFIM given earlier (equation (19)) with the mass Δ replaced by $\Delta(1 + (h/V)^2)$ [41]. From this result, the authors of [19] concluded that the dispersion in the transverse directions in the ordered phase and close to the QCP is much stronger than that deep in the ordered phase.

To calculate the T_c for the case of $g = 0$, we use $\chi_{1D}(\omega = 0, k = 0)$ at finite T

$$\chi_{1D}(\omega = 0, k = 0) = \frac{c_2}{V}\left(\frac{2\pi T}{V}\right)^{-7/4} \tag{23}$$

where the constant $c_2 = \sin(\pi/8)\mathrm{B}^2(1/16, 7/8)$ and $\mathrm{B}(x, y)$ is the Euler beta function. Thus, we find, by using equation (20)

$$\frac{T_c}{V} = c_3 \left(\frac{z_\perp t_\perp}{V}\right)^{4/7} \tag{24}$$

where the constant $c_3 = c_2/(2\pi) = 2.12$. Further, we can also compute the susceptibility χ for the coupled system at the QCP for small $\vec{k}_\perp$ by using the relation for the slightly off-critical χ_{1D} given earlier, equation (19), together with the relation $\Delta_c^2 = g_c^{1/4} V t_\perp$ in equation (17), giving

$$\chi(\omega, k, \vec{k}_\perp) \sim \frac{Z_0 V g_c^{1/4}}{\omega^2 - (vk)^2 - (\vec{v}_\perp \cdot \vec{k}_\perp)^2}, \tag{25}$$

where $|\vec{v}_\perp|^2 = (Z_0 V g_c^{1/4}/2)\mathrm{d}^2 t_\perp(\vec{k}_\perp = 0)/\mathrm{d}\vec{k}_\perp^2$ is gained by a Taylor expansion to second order [19]. Further, the shape of the phase boundary at low T can be determined by using the χ_{1D} of the TFIM at low T [1]

$$\chi_{1D}(\omega, k) = \frac{Z_0(\alpha\Delta/v)^{1/4}}{(\omega + \mathrm{i}/\tau_\psi)^2 - (vk)^2 - \Delta^2}, \tag{26}$$

where $\tau_\psi = \frac{\pi}{2T}\mathrm{e}^{\Delta/T}$ is the dephasing time due to quantum fluctuations. Then, for $\omega = 0 = k$ in χ_{1D}, the equation (20) gives

$$\ln T - \frac{\Delta}{T} = \ln m + \ln \Lambda, \tag{27}$$

where $\Lambda = \frac{\pi}{2}(\frac{Z_0 t_\perp}{g^{7/4} V} - 1)^{1/2}$. The expression (27) given above has an approximate solution [19]

$$T_c = \frac{\Delta}{\ln(1/\Lambda) - \ln\ln(1/\Lambda)}\,. \tag{28}$$

This relation gives us the shape of the phase boundary for low T and close to the QCP. In this way, we have derived the key features of the T–g phase diagram for the case of the $t_\perp$ transverse coupling (figure 4) given above. We can also carry out an identical RPA calculation for the other transverse coupling, $U_\perp$, for the case when the single chain system is critical, $2t = V, t_\perp = 0$ in equation (11) [19]. This is because this theory is again known to be integrable [40] and falls in the same universality class as that of the TFIM. We can thus determine an identical set of relations for (i) the critical coupling g_c at $T = 0$, (ii) the critical temperature T_c for the case of $g = 0$, (iii) the susceptibility χ, (iv) dispersion in the transverse directions as well as (v) the shape of the phase boundary close to the QCP from those obtained earlier, but with $t_\perp$ replaced by $U_\perp$ everywhere. In this way, we obtain essentially the same T–g phase diagram for the case of the $U_\perp$ transverse coupling, with the only difference being the fact that the spectrum of the ordered phase is now obtained from the solution of the critical 1D TFIM in a longitudinal field [40].

We can see from the results given above that, as we move along the interior of the ordered phase towards the phase boundary, the excitation gaps decrease together with a gradual growth of the dispersion in the transverse directions. At the QCP, the spectrum is gapless and this is reflected in the fact that the dynamical susceptibility χ at the QCP can have at most logarithmic corrections. At low T, directly in the region above the QCP, the spectrum and dynamics are mainly governed by the quantum critical point while the thermal excitations are described by the associated continuum quantum-field theory. By this we mean that for energy scales given by $\omega \gg k_B T$, the system still resembles a quantum critical one in this region of the phase diagram while for $\omega \ll k_B T$, a relaxation of the dynamics (given by τ_ψ^{-1}) caused by quantum fluctuations sets in. The rapid growth of the dispersion in the transverse directions close to the QCP is the physics of the dimensional crossover in this system, while the vanishing of all mass gaps at the QCP is the physics of deconfinement. These results echo our earlier finding of the critical phase in the phase diagram of the two-leg TFIM system by starting from the $\tilde{V}$ ordered phase and increasing $t_\perp$. While the integrability of the TFIM allows us to make considerable progress in computing various quantities, the role of the QCP in the mechanism responsible for the dimensional crossover and deconfinement appear to be robust. These results lead us, therefore, to the conclusion that critical quantum fluctuations associated with a QCP can quite generically cause such critical (gapless) phases to emerge in higher dimensions from the ordered (gapped) phases of lower-dimensional systems when coupled to one another.

4. Comparison with recent numerical works

We present here a brief discussion of the relevance of our work to some numerical investigations that have been carried out on two-leg ladder systems as well as coupled TFIM systems. Vojta *et al* [42] studied the problem of a strongly correlated electronic problem at 1/4-filling and with extended Hubbard interactions (keeping only an nn repulsion) using the DMRG method. The phase diagram they obtained contains several phases with charge and/or spin excitation gaps. While a comparison of our work with this study is hindered by the fact

that the DMRG analysis does not have the crucial element of the nnn repulsion (V_2 in our work), figure 2 of that work reveals that for the case of $U \gg V_1 > t$, the authors indeed find a charge-ordered CDW state (i.e. the Wigner charge-ordered state of [12]) with an excitation gap in the spin sector as well. This is in conformity with our finding of a Wigner charge-ordered state with a spin gap for the case of the U_ρ coupling being the most relevant under RG. Further, the $t_\perp$ of that study corresponds to the single-particle hopping between the legs while our work has focused on the effects of two-particle hopping. Finally, with the on-site Hubbard coupling, U, being the largest in the problem, we are unable to see any phase-separated state in our phase diagram (as observed by Vojta *et al*).

In a slightly earlier work, Riera *et al* [43] studied the case of 1/4-filled chain/ladder Hubbard and t–J systems, but which also include Holstein and/or Peierls-type couplings to the underlying lattice. Their findings reveal co-existing charge and spin orders in both chain and ladder systems. Specifically, for the case of their chain system, by keeping only on-site and nn repulsion together with an on-site Holstein-type coupling of the electronic density to a phonon field, their phase diagrams (figures 4) reveal separate phases with Wigner as well as Peierls-type charge order. This is in keeping with our findings, but the origins of the Peierls order in the two cases are different: in our work, it originates from the competition of the nnn coupling V_2 with the nn coupling V_1, while in their work, it needs the Holstein coupling to the lattice. Riera *et al* find a similar phase diagram (figures 5) for the case of an extended t–J model (i.e. including nnn t and J couplings) with a Holstein coupling. The addition of a Peierls-type coupling leads to a spin-Peierls instability, i.e. the formation of a dimerized spin order, which coexists with the Peierls-type charge order. Again, while this matches our findings, the origins are different. Qualitatively similar conclusions are also reached by the authors in their study of an anisotropic two-leg t–J ladder with an extended on-chain nn coupling and Holstein-/Peierls-type lattice couplings (figures 2 and 3).

Finally, we comment on the very recent DMRG studies of Konik *et al* [44] on coupled TFIM systems in an effort at studying 2D coupled arrays of 1D systems. By starting with a reliable spectrum truncation procedure for a single TFIM chain (which relies on the underlying continuum 1D theory being either conformally invariant or gapped but integrable), the authors then implement an improvement of their DMRG algorithm using first-order perturbative RG arguments. Their results for a $U_\perp$ coupling of the TFIM chains confirms the accuracy of the RPA analysis of [19] and the present work in computing quantities like the single chain excitation gap (which is found to vanish at a critical $U_\perp$) and dispersion of excitations in the coupled system as a function of $U_\perp$. Their results indicate that the RPA method and the DMRG analysis agree very well up to values of $U_\perp$ of the order of the gap. This method also appears to give accurate values of critical exponents related to the ordering transition. Thus, this numerical approach appears to provide a confirmation of the interplay of the QCP in the TFIM and the transverse coupling in driving the dimensional crossover and deconfinement transition. Such an approach, therefore, holds much promise for the numerical investigations of such phenomena in systems with similar ingredients.

5. Conclusions

To conclude, we have studied a model of strongly correlated coupled quasi-1D systems at 1/4-filling using an effective pseudospin TFIM model. Using a bosonization and RG analysis for a two-leg ladder model, we find two different types of charge-/spin-ordered ground states at 1/4-filling. Transverse bond-fermion hopping is found to stabilize a new, gapped (insulating) phase characterized by interchain two-particle coherence of a type resembling orbital antiferromagnetism [29, 18]. The spin fluctuations are described by a $S = 1/2$ Heisenberg ladder-type model for all cases studied here: the spin excitations are always massive. Away from this filling, either intra-or interchain superconductivity in a gapped spin background is found to be the stable ground state. We also find the existence of an intermediate gapless phase lying in between two gapped, charge-ordered phases (characterized by the relevant couplings $\tilde{V}$ and $t_\perp$ respectively) in the RG phase diagram of our model.

We followed this up with an RPA analysis of the case when many such effective TFIM systems are coupled. We find that a transverse bond-fermion (i.e. two-particle) hopping coupling causes the ordered phase to extend to finite temperatures, with the phase boundary ending at a $T = 0$ QCP. Interestingly, the critical quantum fluctuations at the QCP, together with the transverse coupling $t_\perp$, are found to drive a deconfinement transition (at $T = 0$) together with a dimensional crossover characterized by strong dispersion of the excitations of any single TFIM into the transverse directions. The gapless higher-dimensional system in the quantum critical region lying just above the QCP is in conformity with our finding of a critical phase in the two-leg ladder model driven by $t_\perp$ discussed above. Similar conclusions are also reached for the effects of the transverse coupling $U_\perp$ on effective TFIM chains which are critical. The mechanism driving the dimensional crossover and deconfinement appear to be generic and lead us to believe that a similar mechanism should exist for the case of other quantum critical systems in lower dimensions when coupled to one another. Our present analyses are, however, especially relevant to coupled chain systems like the TMTSF organic systems as well as coupled ladder systems like $Sr_{14-x}Ca_xCu_{24}O_{41}$ and α-NaV_2O_5 or β-$Na_{0.33}V_2O_5$ (a superconductor) which exhibits charge/spin long-range order at $x = 0$ and superconductivity beyond, under pressure and/or doping [2, 3].

Acknowledgments

SL and MSL thank the ASICTP and MPIPKS respectively for financial support. SL thanks F Franchini, L Dall'Asta, S Basu, S T Carr, M Fabrizio and A Nersesyan for many discussions.

References

[1] Sachdev S 1999 *Quantum Phase Transitions* (Cambridge: Cambridge University Press) and references therein
[2] McCarron E M III *et al* 1988 *Mater. Res. Bull.* **23** 1355

Uehara M *et al* 1996 *J. Phys. Soc. Japan* **65** 2764
[3] Yamauchi T, Ueda T and Mori N 2002 *Phys. Rev. Lett.* **89** 057002
[4] Giamarchi T 2004 *Quantum Physics in One Dimension* (Oxford: Oxford University Press) and references therein
[5] Capponi S, Poilblanc D and Giamarchi T 2000 *Phys. Rev.* B **61** 13410
[6] Thalmeier P and Fulde P 1998 *Europhys. Lett.* **44** 242
[7] Mostovoy M V and Khomskii D I 2000 *Solid State Commun.* **113** 159
[8] Aichhorn M, Horsch P, von der Linder W and Cuoco M 2002 *Phys. Rev.* B **65** 201101
[9] Abbamonte P *et al* 2004 *Nature* **431** 1078 and references therein
[10] Jerome D 1994 *Organic Superconductors: From* $(TMTSF)_2PF_6$ *to Fullerenes* (New York: Dekker) p 405
[11] Emery V J and Noguera C 1988 *Phys. Rev. Lett.* **60** 631
[12] Laad M S and Lal S 2005 *Preprint* cond-mat/0510016
A comprehensively extended work is presented in *Preprint* 0708.2156 [cond-mat]
[13] Yoshioka H, Tsuchiizu M and Seo H 2006 *J. Phys. Soc. Japan* **75** 063706
[14] Yoshioka H, Tsuchiizu M and Seo H 2007 *Preprint* 0708.0910 [cond-mat]
[15] Donohue P, Tsuchiizu M, Giamarchi T and Suzumura Y 2001 *Phys. Rev.* B **63** 045121
[16] Orignac E and Citro R 2003 *Eur. Phys. J.* B **33** 419
[17] Carr S T and Tsvelik A M 2002 *Phys. Rev.* B **65** 195121
[18] Gogolin A O, Nersesyan A A and Tsvelik A M 1998 *Bosonization and Strongly Correlated Systems* (Cambridge: Cambridge University Press) and references therein
[19] Carr S T and Tsvelik A M 2003 *Phys. Rev. Lett.* **90** 177206
[20] Schulz H J 1996 *Phys. Rev. Lett.* **77** 2790
[21] Lieb E, Schultz T and Mattis D 1961 *Ann. Phys.* **16** 406
[22] Niemeijer Th 1967 *Physica* **36** 377
Niemeijer Th 1968 *Physica* **39** 313
[23] Chakrabarti B K, Dutta A and Sen P 1996 *Quantum Ising Phases and Transitions in Transverse Ising Models* (*Lecture Notes in Physics* vol m 41) (Berlin: Springer)
[24] Kopp A and Chakravarty S 2005 *Nat. Phys.* **1** 53
[25] Schulz H J 1986 *Phys. Rev.* B **34** 6372
[26] Ho A F, Cazalilla M A and Giamarchi T 2004 *Phys. Rev. Lett.* **92** 130405
Ho A F, Cazalilla M A and Giamarchi T 2006 *New J. Phys.* **8** 158
[27] Benfatto L, Castellani C and Giamarchi T 2007 *Phys. Rev. Lett.* **98** 117008
[28] Japaridze G I and Nersesyan A A 1978 *Sov. Phys.—JETP Lett.* **27** 334
Pokrovsky V L and Talapov A 1979 *Phys. Rev. Lett.* **42** 65
[29] Kusmartsev F V, Luther A and Nersesyan A A 1992 *JETP Lett.* **55** 692
[30] Dutta A and Sen D 2003 *Phys. Rev.* B **67** 094435
[31] Affleck I and Halperin B I 1996 *J. Phys. A: Math. Gen.* **29** 2627
[32] Scalapino D J, Imry Y and Pincus P 1975 *Phys. Rev.* B **11** 2042
[33] Bocquet M, Essler F H L, Tsvelik A M and Gogolin A O 2001 *Phys. Rev.* B **64** 094425
[34] Giamarchi T and Tsvelik A M 1999 *Phys. Rev.* B **59** 11398
[35] Starykh O A and Balents L 2004 *Phys. Rev. Lett.* **93** 127202
[36] Irkhin V Y and Katanin A A 2000 *Phys. Rev.* B **61** 6757
[37] Bocquet M 2002 *Phys. Rev.* B **65** 184415
[38] Arrigoni E 2000 *Phys. Rev.* B **61** 7909
Biermann S, Georges A, Lichtenstein A and Giamarchi T 2001 *Phys. Rev. Lett.* **87** 276405
[39] Itzykson C and Drouffe J-M 1989 *Statistical Field Theory* vol 1 (Cambridge: Cambridge University Press)
[40] Zamolodchikov A B 1988 *Int. J. Mod. Phys.* A **3** 743
[41] Delfino G, Mussardo G and Simonetti P 1996 *Nucl. Phys.* B **473** 469
[42] Vojta M, Hübsch A and Noack R M 2001 *Phys. Rev.* B **63** 045105
[43] Riera J and Poilblanc D 1999 *Phys. Rev.* B **59** 2667
[44] Konik R M and Adamov Y 2007 *Preprint* 0707.1160 [cond-mat]